IS-PORTO 2023 PROCEEDINGS

Proceedings of the 8th International Symposium on Deformation Characteristics of Geomaterials
3rd - 6th September 2023

Please indicate your preference for paper publication:
ASTM Geotechnical Testing Journal Special Issue ☐
Symposium Proceedings ☒

Freezing-thawing response of sand-kaolin mixtures in oedometric conditions

Andrea Viglianti[1#], *Giulia* Guida[1], and *Francesca* Casini[1]

[1]*Università degli studi di Roma Tor Vergata, Dipartimento di Ingegneria Civile e Ingegneria Industriale, via del Politecnico 1 Rome 00133, Italy*
[#]*Corresponding author: andrea.viglianti@uniroma2.it*

ABSTRACT

Freezing and thawing cycles applied to soils can be often causes of irreversible instabilities, uplift, or subsidence. These phenomena can be both naturally (*e.g.* permafrost regions) or artificially induced (*e.g.* artificial ground freezing, as an excavation earth support technique for tunnelling). When soil temperature falls below 0°C, the pore liquid water changes phase turning into ice. The freezing process generally implies an expansion of the soil element due to: (i) the lower density of the ice and (ii) the pore water migration towards the frozen front. The complex interaction existing between the solid grains, the water and the ice formation during freezing determines the overall thermo-hydro-mechanical behaviour of the soil. Sandy mixtures with different percentages of kaolin were tested in an oedometer developed at the Geotechnical Laboratory of Università degli Studi di Roma Tor Vergata, working with temperature below zero. The samples were compressed at five maximum vertical stresses (50, 100, 200, 400 and 800 kPa, respectively), and then a freezing and thawing cycle was applied by step down to a minimum temperature of -20°C. The experimental results in terms of the evolution of temperature, vertical displacements and liquid water monitored are discussed and interpreted by means of a micro-to-macro approach. Interesting outcomes characterising the mechanical and hydraulic hysteresis during freezing and thawing processes emerged from the data analysis. A deeper understanding of the coupled phenomena occurring during freezing and thawing cycles is supposed to provide an important contribution to the development of a constitutive model able to reproduce the irreversible volumetric response of frozen soils.

Keywords: AGF, frost-heave; THM phenomena; freezing thawing cycle.

1. Introduction

When the soil is subjected to freezing and thawing process, it may undergo to relevant volume and stiffness variation inducing possible lack of service to structures and infrastructure at the ground surface.

In cold regions, the shallow layer of ground is subjected to cycles of freezing and thawing in response to the seasonal air temperature that fluctuates above and below 0°C during the year (Andersland *et al.*, 2004). Many damages associated with frost heave and thawing settlement have been recorded in lined canals (Li *et al*. 2019), or in highway and railway in cold region around the world (Li *et al*, 2008). The displacements depends by the soil type, the depth of frost penetration, the water availability, the territory topology (Daout *et al.*, 2017) and the magnitude and duration of freezing temperature.

Indeed, the temperature cycle applied can be non-natural due to the artificial ground freezing (AGF) technology. It is an excavation earth supporting technique generally adopted in critical situations such as urban excavation under the water table level in coarse grained soils (Viggiani and Casini, 2015). Toledo station of Naples underground is an important historical case of AGF's application. Relevant settlements (larger than three times the maximum heave recorded during the freezing stage) are there observed at the foundation plane of a building over the tunnel excavated (Russo *et al*., 2015).

Freeze-thaw cycles are known to induce irrecoverable volume change especially in fine-grained soils (Nishimura, 2021). When a wet soil is subjected to a freezing process, a volume expansion can be generally observed. The increase of volume is not only due to the different densities of liquid water and ice, but mainly (in fine-grained soils) to a water migration process towards the frozen front (Talamucci, 2003). This may lead to the formation of ice lenses, thus the formation of sequence of pure ice layers alternating with regions of completely frozen soils (Rempel, 2007).

During thawing, the soil is usually subjected to a shrinkage. The ice disappears and the soil skeleton reaches a new equilibrium configuration characterised by a new void ratio. The amount of water drained during thawing depend on the permeability and on the stiffness of the soil (Andersland *et al*., 2004).

Several authors have investigated the mechanical behaviour of soils subjected to thermal loading in laboratory-controlled conditions. Dalla Santa *et al* (2016) have carried out oedometric tests in which the specimen, under vertical constant stress, has been subjected to cyclic thermal stress (two different cyclic temperature intervals: -5 °C ÷ +15 °C and -5 °C ÷ +50 °C) to investigate the compressibility of silty and cohesive sediments. A significant and irreversible settlement has been observed at the end of the thermal cycles. Peláez *et*

al. (2014) tested the Pozzolana and Neapolitan Yellow Tuff on freezing and thawing cycles applying the temperatures of +22 °C and -20 °C at constant vertical stress and under oedometric condition. The accumulation of irreversible volumetric deformation has increased with the number of cycles and with the decrease of vertical stress for both the material investigated.

In this work, an oedometric apparatus able to apply freezing and thawing cycles was modified to test samples of sand with different percentage of kaolin under given vertical stress. In the following, are reported the details of the oedometric apparatus modifications, the material, the tests performed and the analysis of the results.

2. The experimental apparatus

An oedometric cell developed for unsaturated soils has been modified to work with temperature below zero (Pelaez *et al*., 2014). The air drains transducers were closed (see Figure 1.a). The thermal loading is applied by immerging the oedometric cell in a thermostatic bath constituted by a mixture of water (50 %) and glycol (50 %) that, refrigerated by a cryostat, can achieve temperatures below 0°C without changing phase. The oedometer is positioned on a supporting frame (in red, see Figure 1.b) to keep the top of the loading head emerged and to avoid damages on the displacement transducer. The system is insulated from the environment through piral panels (Figure 1.c). The temperature inside the specimen is monitored by a thermocouple inserted in the central part of the oedometer cell (Figure 1.d).

The oedometric cell hosts a cylindrical specimen with a diameter of 5 cm and a height of 2.0 cm. The vertical load is applied through compressed air at the top of the specimen and kept constant for each thermal loading cycle. The water drainage is placed at the bottom of the specimen and connected to a reservoir. During the test, the vertical displacement was measured by a LVDT connected to the head of the oedometer. The amount of drained water is measured with a water volume gauge. Finally, the temperature is monitored with a thermocouple reported in Figure 1.d. The amount of liquid water drained can be measured until the water in the tube freezes.

Calibration tests of the apparatus are in progress to purify the measurements from system deformations.

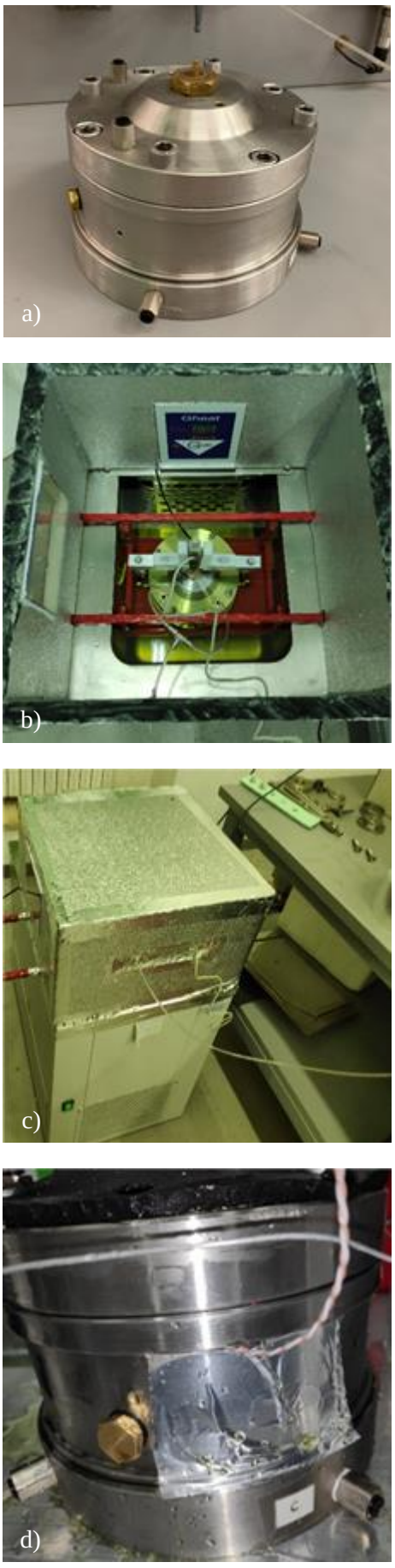

Figure 1. Experimental apparatus: (a) original oedometric cell; (b) thermostatic bath; (c) insulation system; (d) thermocouple.

3. Materials and experimental campaign

Materials tested are mixtures of Fontainbleau sand and Kaolin Speswhite, representative of intermediate soils, such as alluvial deposits in Rome, where several interventions of artificial ground freezing will be adopted for the Metro C tunnelling excavation (Metro C S.C.p.A.). The sand is characterized by grain size between 100 and 400 μm, the kaolin particles have a diameter < 2 μm with a specific gravity G_s = 2.65. The following three different mixtures were investigated at increasing percentage of kaolin content:

- S100K0: 100 % sand and 0 % kaolin
- S90K10: 90 % sand and 10 % kaolin
- S80K20: 80 % sand and 20 % kaolin.

Figure 2 shows optical microscope images with magnification 40x of the mixtures adopted. The preparation of S100K0 consisted in mixing 65 g of sand with 13.25 g of water. The S90K10 and S80K20 specimens were prepared by mixing sand and kaolin for few minutes, and then adding water. From the images it emerges how the kaolin fits the interparticle space between the sand grains. The tests started after one day from the packing, to allow the homogenization of the degree of saturation (S_r = 90 %).

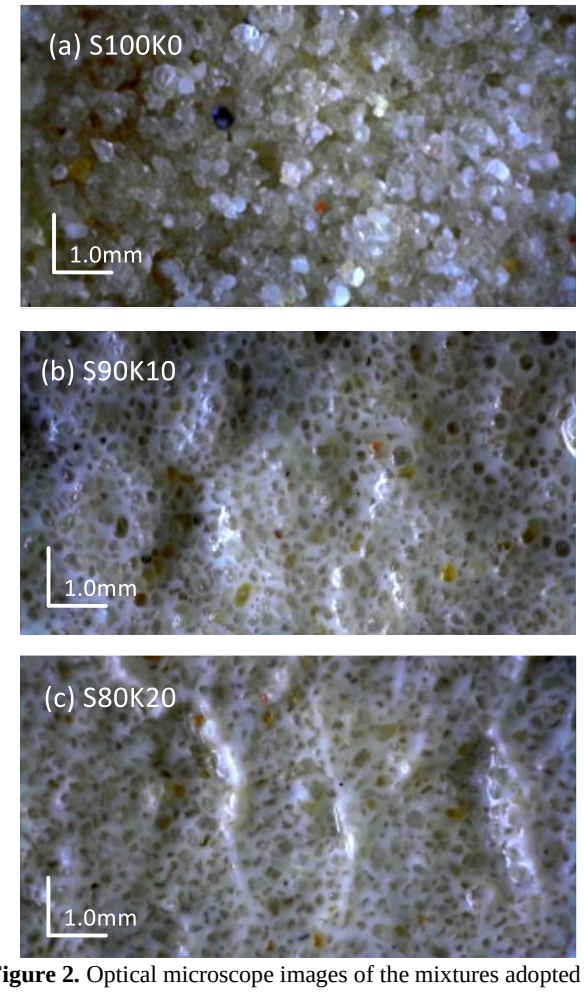

Figure 2. Optical microscope images of the mixtures adopted (Magnification 40x)

The tests phases are the following: (i) saturation, (ii) vertical compression and (iii) freezing-thawing (F-T) cycles. The saturation occurred imposing a back pressure of p_w=20 kPa and a vertical effective stress of σ'_v = 25 kPa. The vertical compression was applied by steps up to the predefined vertical effective stress (50 – 800 kPa). The consolidation time increased with the fine content: two hours for the S100K0 specimen and three to six hours for the other samples. Figure 3 shows the freezing and thawing cycle imposed in terms of the evolution of temperature with time.

Each target temperature is maintained for 300 min and its change ΔT was applied in 60 min. In between the temperatures 0 °C and -2 °C, the imposed variation of temperature is small ΔT = -0.5 °C to study the effects of the ice-formation. In the range of temperatures from -2°C to - 10°C, the step of temperature variation increased to ΔT = -8 °C, and the last decrease of temperature is ΔT= -10 °C down to -20°C. The thawing process follows the same path in the opposite direction (Figure 3).

At the end the freezing-thawing cycle the samples were unloaded until the initial effective stress of σ'_v = 25 kPa.

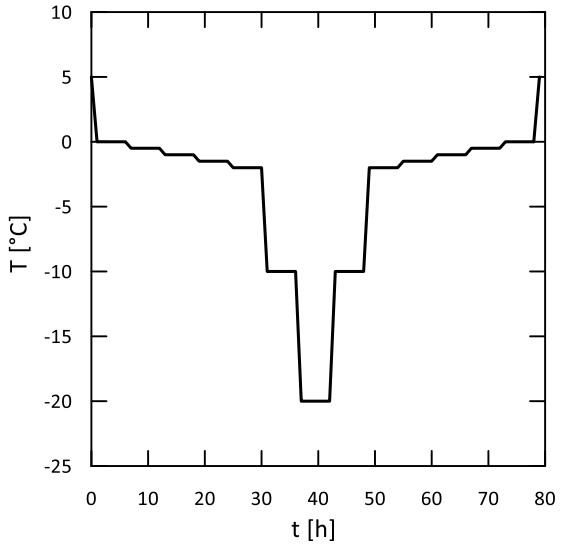

Figure 3. Evolution of temperature during a freezing-thawing cycle.

4. Results

In this work, are reported the experimental results of the three mixtures with a vertical stress applied of 200 kPa.

4.1. Mechanical response

Figure 4 reports the compression curves, in the $e - \log(\sigma'_v)$ plane. The initial void ratio differs between the three mixtures due to the phase preparation and saturation of the specimens. The pure sand mixture S100K0 shows the loosest density (e_0~0.67). Sand-kaolin mixtures show a lower initial void index than sand, although unexpectedly higher for S80K20 than for S90K10. This is probably a result of the saturation phase that induces greater compaction for a lower content of kaolin (S10K90).

The loading path up to σ'_v = 100 kPa of vertical stress was sub-horizontal for all the specimens investigated. Then, the sand-kaolin mixtures yielded at a vertical stress in between 100 and 200 kPa, while the pure sand

(S100K0) maintained an elastic and stiff response until 200 kPa. The volumetric compaction during the loading path increased according to the fine content (Δe ~-0.06 for S90K10 and Δe ~-0.11 for S80K20).

After the freezing-thawing cycle, all specimens showed differential displacements (orange branch in Figure 4): the pure sand specimen swells (a slight positive variation of void ratio is observed), while the mixtures with kaolin further compact as much as greater is the percentage of fine content.

During the unloading phase, the mixtures exhibited a stiff behavior characterized by Cs ≈ 0.

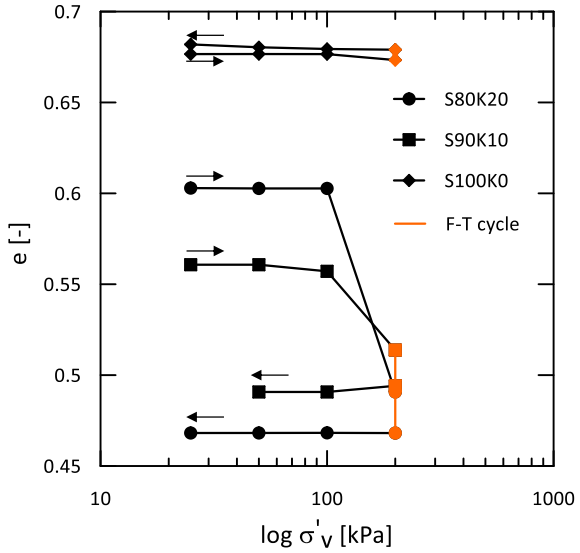

Figure 4. Compression curves for the three mixtures analysed during the loading, freezing and thawing cycle, and unloading path.

4.2. Effects of temperature

To deeper understand the irreversible response induced by the FT cycle, the measured axial strain during F-T cycle is plotted against the temperature in Figure 5.

During freezing (blue curve from right to left), all samples explicated negative axial strain related to swelling, with the magnitude that increases with the fine content, from a value of $\varepsilon_a = -0.75\,\%$ for S100K0 to $\varepsilon_a = -1.25\,\%$ for S80K20. Most of the sweeling behaviour occurred in the range of temperature between 0°C and -10°C.

During thawing (red curve to from left to right), the curve overlapped the freezing path up to -10°C and it is almost constant up to - 2°C. Then, it rapidly increased in between -2°C and 5°C showing a residual negative axial deformation in the case of pure sand ($\varepsilon_{a,final} \sim -0.3\,\%$ S100K0). Further, a positive values of axial deformation (shrinkage) is recorded of $\varepsilon_{afinal} \sim 1.13\,\%$ for S90K10 and of $\varepsilon_{afinal} \sim 1.5\,\%$ for S80K20.

Thus, a systematic hysteresis is observed in the three mixtures investigated. After the thermal cycle, the soil skeleton achieves a new equilibrium configuration characterized depending of the overburden stress applied and the grain size distribution (Andersland *et al.*, 2004).

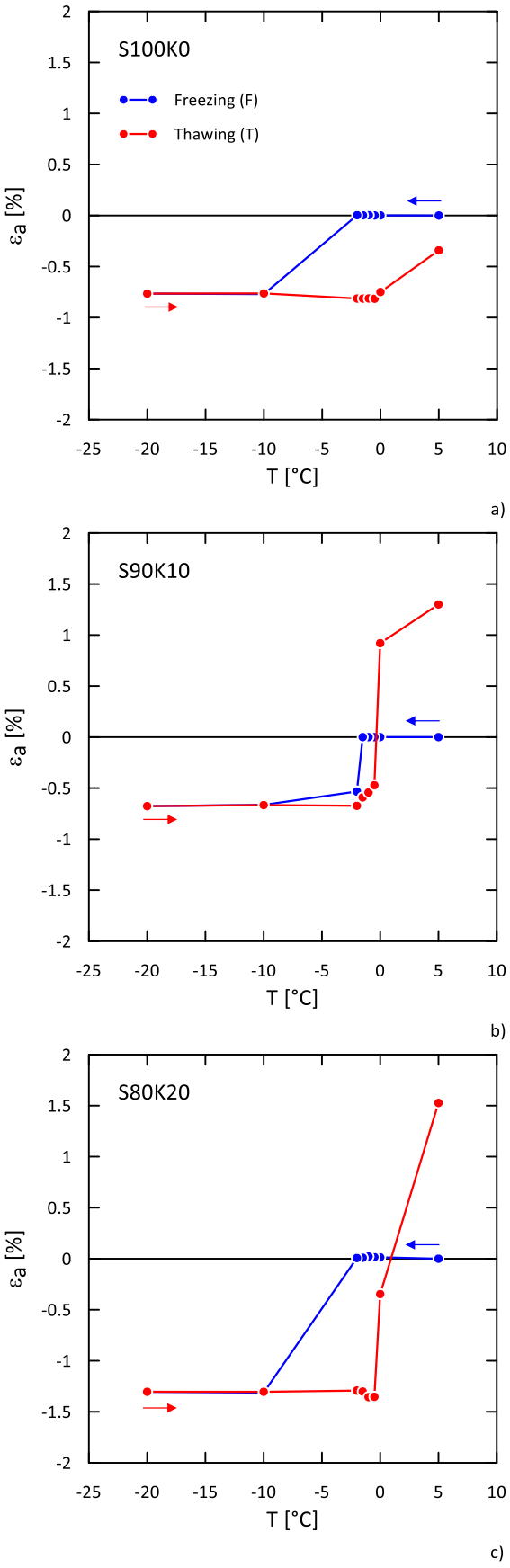

Figure 5. Evolution of axial strain with temperature.

4.3. Water migration

The volume of water drained by the specimens during the whole test was measured by a volume gage (capacity 40 ml) placed outside the cryostat. Figure 6 reports the

evolution of the "water deformation" ε_w (= $\Delta V_w/V_0$) with temperature. When ε_w is positive, the water is drained by the sample, and negative is absorbed.

During freezing (blue curves from right to left) a first slightly water inflow towards the specimen was recorded between 0°C and -1°C, especially for the mixtures S100K0 and S90K10 (Figure 6.a, b). As the temperature further decreased all the mixtures expelled water, especially between -1°C and -3°C, achieving a value of $\varepsilon_w \approx 1$ % when T = -20 °C. The water drains during freezing because the ice phase displaces the liquid water.

During thawing (red curves from left to right), ε_w remained constant up to T = -2 °C, then it rapidly increased. The water drainage upon thawing increases with the fine content (Figure 6).

Figure 7 reports the variation with the temperature of the ice ratio Δe_i defined as:

$$\Delta e_i = -(\epsilon_v - \epsilon_w)(1 + e_0) \quad (1)$$

where, e_0 is the void ratio at 0 °C (before cycle), ϵ_v the volumetric deformation, with $\epsilon_v = \epsilon_a$ in oedometric conditions. The variation of ice ratio corresponds to the amount of water transforming into ice. During freezing (blue curve from right to left) the temperature at which Δe_i increases depends on the type of mixture. Thus, the ice-formation temperature decreases with the increasing fine content. The amount of ice developed is mostly influenced also by the initial void ratio: the pure sand mixture S100K0, characterized by the higher initial void ratio achieved a $\Delta e_i \sim 0.04$ during the freezing phase, while the mixture S90K10, characterized by a denser initial state, achieved $\Delta e_i \sim 0.028$. In addition, the mixture S90K10 already at -2°C develops almost the entire ice formation, while S100K0 and S80K20 needed lower temperatures. Further, also the ice ratio exhibit a hysteresis, the melting process required greater temperatures to occur than the freezing (see the thawing paths in Figure 7). The melting of ice just around -0.5°C for the three mixtures tested.

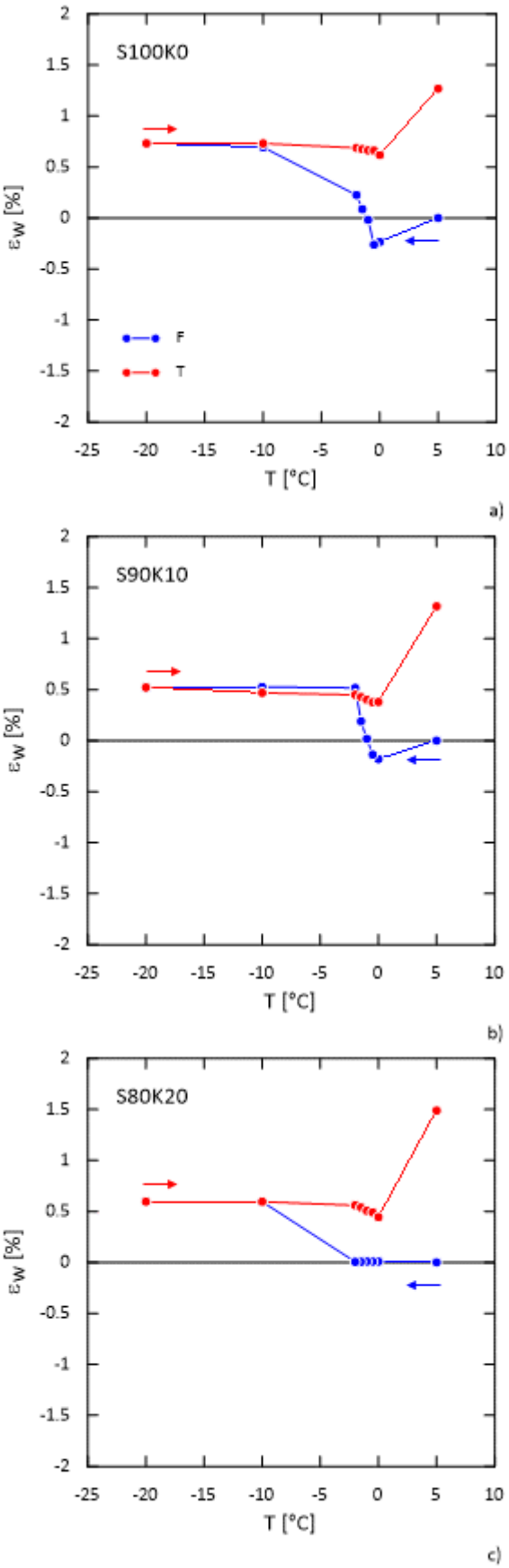

Figure 6. Evolution of water deformation with temperature for the three mixtures analysed.

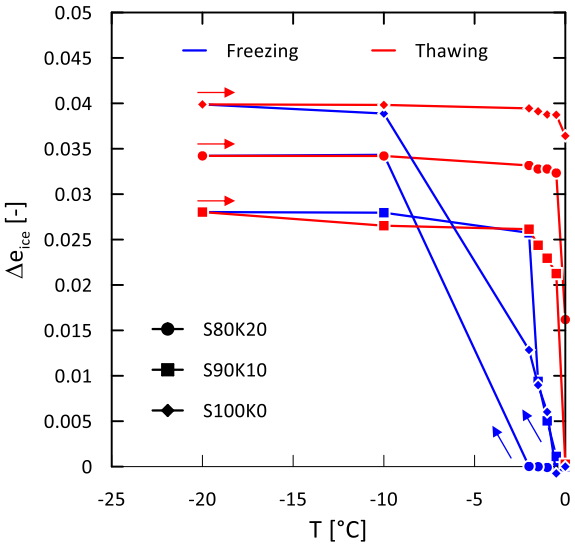

Figure 7. Variation of void ratio and water ratio with temperature.

5. Conclusion

This paper reported the preliminary oedometric results obtained on frozen samples under constant vertical stress. Three sandy specimens, with different percentage of fine content, were tested under 200 kPa of vertical effective stress and during a freezing-thawing cycle between 5 °C and -20°C. The quantities monitored during the tests are in terms of axial displacement, water volume change and temperature inside the specimen. The response in terms of axial deformation is systematically irreversible, with the tendency of a residual swelling in the case of pure sand and of a residual soil compaction for the increasing fine content. The greater the fine content, the greater is the entity of deformation during both freezing (swelling) and thawing (compaction). The irreversibility of the freezing-thawing process is due to the hysteresis of the freezing retention curve and its coupling with the mechanical behaviour.

Additional tests will be at different vertical load applied and with different thermal load rate. Calibration tests of the apparatus are in progress to purify the measurements from system deformations.

Acknowledgements

Andrea Viglianti knowledge the Ministry of Economic development for the support with the Proof of Concept – FROZEN GeoLab project.

Giulia Guida obtained the financial support of the Regione Lazio through POR-FSE 2014/20 Contributions for the permanence of excellence in the academic world, n. 65629/2020.

The authors are grateful to Davide Coluzzi and Marco Amici for their contribution to the apparatus development during their Master thesis.

References

Andersland, O. B., and Ladanyi, B. “Frozen ground engineering”, 2th ed., John Wiley & Sons, Inc., Hoboken, New Jersey, 2004, ISBN 0471615498.

Dalla Santa, G., Galgaro, A., Tateo, F., & Cola, S. “Modified compressibility of cohesive sediments induced by thermal anomalies due to a borehole heat exchanger”, Engineering Geology, 202, 143-152, (2016). https://doi.org/10.1016/j.enggeo.2016.01.011

Daout, S., Doin, M. P., Peltzer, G., Socquet, A., & Lasserre, C., “Large-scale InSAR monitoring of permafrost freeze-thaw cycles on the Tibetan Plateau”, Geophysical Research Letters, 44(2), 901-909, (2017). https://doi.org/10.1002/2016GL070781

Li, N., Chen, F., Xu, B., & Swoboda, G., “Theoretical modeling framework for an unsaturated freezing soil”, Cold Regions Science and Technology, 54(1), 19-35, (2008). https://doi.org/10.1016/j.coldregions.2007.12.001

Li, S., Lai, Y., Zhang, M., Pei, W., Zhang, C., & Yu, F., “Centrifuge and numerical modeling of the frost heave mechanism of a cold-region canal”. Acta Geotechnica, 14(4), 1113-1128, (2019). https://doi.org/10.1007/s11440-018-0710-1

Miao, Q., Niu, F., Lin, Z., Luo, J., & Liu, M., “Comparing frost heave characteristics in cut and embankment sections along a high-speed railway in seasonally frozen ground of Northeast China”, Cold regions science and technology, 170, 102921, (2020). https://doi.org/10.1016/j.coldregions.2019.102921

Metro C S.C.p.A., Avaible at: https://metrocspa.it/lopera/la-tecnica-del-congelamento-artificiale-dei-terreni/ , accessed: 12/10/2022

Nishimura, S., “A model for freeze-thaw-induced plastic volume changes in saturated clays”, Soils and Foundations, 61(4), 1054-1070, (2021). https://doi.org/10.1016/j.sandf.2021.05.008

Peláez, R. R., Casini, F., Romero, E., Gens, A., & Viggiani, G. M. B., “Freezing-thawing tests on natural pyroclastic samples”. Unsaturated Soils: Research & Applications (pp. 1689-1694), CRC Press, (2020). ISBN 9781003070580.

Rempel, A. W., “Formation of ice lenses and frost heave”. Journal of Geophysical Research: Earth Surface, 112(F2), (2007). https://doi.org/10.1029/2006JF000525

Russo G., Corbo A., Cavuoto F. & Autuori S., “Artificial ground freezing to excavate a tunnel in sandy soil. Measurements and back analysis”, Tunnelling and Underground Space Technology, 50, 226-238, (2015). https://doi.org/10.1016/j.tust.2015.07.008

Talamucci, F., “Freezing processes in porous media: formation of ice lenses, swelling of the soil”, Mathematical and Computer Modelling, 37(5-6), 595-602. (2003). https://doi.org/10.1016/S0895-7177(03)00053-0

Thomas, H. R., Cleall, P., Li, Y. C., Harris, C., & Kern-Luetschg, M., “Modelling of cryogenic processes in permafrost and seasonally frozen soils”, Geotechnique, 59(3), 173-184, (2009). https://doi.org/10.1680/geot.2009.59.3.173

Trevi S.p.a. (2013). “Congelamento artificiale dei terreni - tecnologia”, Available at: https://www.trevispa.com/en/Technologies/artificial-ground-freezing , accessed: 01/07/2022.

Viggiani G.M.B. & Casini F., “Artificial Ground Freezing: from applications and case studies to fundamental research”, Geotechnical Engineering for Infrastructure and Development, 65-92. (2015). doi:10.1680/ecsmge.60678.